

## X-ray Emission from Charge Exchange between Low-energy Highly Charged Ions and H Atoms and Its Astronomical Applications

**Authors:** Zhang Chijun, Liao Tian, Zhang Ruitian, Zhu Xiaolong, Guo Dalong, Gao Yong, Xu Shenyue, Zhang Shaofeng, Ma Xinwen, Zhang Ruitian

**Date:** 2023-12-03T00:00:00+00:00

### Abstract

Experimental and theoretical investigations of charge exchange X-rays from low-energy highly charged ions colliding with H atoms provide important atomic data for diagnosing and modeling non-equilibrium plasmas in astrophysical environments. In this work, we employ the semi-classical multi-channel Landau-Zener (MCLZ) method to calculate charge exchange cross sections for bare and hydrogen-like C, N, and O ions with H atoms, and compare them with reported experimental results. We find that for the  $C5+ + H$  collision system, the theoretically calculated total cross sections differ significantly from experimental measurements. We also compare state-selective cross sections calculated by the MCLZ method and the full quantum molecular orbital close-coupling (QMOCC) method within the solar wind ion velocity (or energy) regime. We find that for charge exchange into  $n = 3$ , the MCLZ state-selective cross sections increase with collision energy, while for charge exchange into  $n = 4$ , they decrease with collision energy; at the low-energy end, they are smaller than the QMOCC results by as much as two orders of magnitude. Finally, using the Kronos package developed in the astrophysics community, we calculate the charge exchange X-ray spectrum, line intensity ratios, and hardness ratio for  $O8+ + H$  at 1000 eV/u using Janev's recommended cross-section data, and compare them with MCLZ calculations. We conclude that the large errors in MCLZ calculations will affect accurate modeling of astrophysical environments. There is an urgent need to develop more accurate full quantum theories.

## Full Text

# X-ray Emission Following Charge Exchange Between Low-Energy Highly Charged Ions and H Atoms and Its Astrophysical Applications

Chijun Zhang<sup>1,2</sup>, Tian Liao<sup>3</sup>, Ruitian Zhang<sup>1,2</sup>, Xiaolong Zhu<sup>1,2</sup>, Dalong Guo<sup>1,2</sup>, Yong Gao<sup>1,2</sup>, Shen Yue Xu<sup>1,2</sup>, Shaofeng Zhang<sup>1,2</sup>, Xinwen Ma<sup>1,2</sup>

<sup>1</sup> Institute of Modern Physics, Chinese Academy of Sciences, Lanzhou 730000, China;

<sup>2</sup> University of Chinese Academy of Sciences, Beijing 100049, China;

<sup>3</sup> Sino-French Institute of Nuclear Engineering and Technology, Sun Yat-sen University, Zhuhai 519082, China)

**Abstract:** Experimental and theoretical investigations of X-ray emission following charge exchange between low-energy highly charged ions and atomic hydrogen provide crucial atomic data for diagnosing and modeling non-equilibrium plasmas in astrophysical environments. In this work, we employ the semiclassical multi-channel Landau-Zener (MCLZ) method to calculate total charge exchange cross sections for bare and hydrogen-like C, N, and O ions colliding with H atoms, and compare these with existing experimental results. We find that for the  $C^{5+} + H$  collision system, the theoretically calculated total cross sections differ significantly from experimental measurements. We also compare state-selective cross sections computed using the MCLZ method and the fully quantum-mechanical molecular orbital close-coupling (QMOCC) method within the solar wind ion velocity (or energy) range. For capture into the  $n = 3$  shell, the MCLZ state-selective cross sections increase with collision energy, while for capture into  $n = 4$ , they decrease with collision energy, being up to two orders of magnitude smaller than QMOCC results at low energies. Finally, using the Kronos program package developed for astrophysical applications, we calculate the charge exchange X-ray spectrum, line intensity ratios, and hardness ratio for 1000 eV/u  $O^{8+} + H$  using the recommended cross sections from Janev [1], and compare these with MCLZ calculations. We conclude that the MCLZ method exhibits large uncertainties that can affect accurate modeling of astrophysical environments, necessitating the development of more accurate fully quantum theoretical approaches.

**Keywords:** low-energy highly charged ions; charge exchange; X-ray; astrophysical plasma

Received date: 2023-11-29; Revised date: 2023-11-29

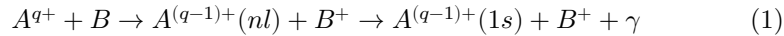
Foundation item: National Key Research and Development Program of China (2017YFA0402400 and 2017YFA0402300)

Corresponding author: Ruitian Zhang, E-mail: zhangrt@impcas.ac.cn

Corresponding author: Xinwen Ma, E-mail: x.ma@impcas.ac.cn

In collisions between low-energy highly charged ions and neutral atoms or

molecules, the process where electrons from the target are captured by the projectile ion is known as charge exchange, electron capture, or charge transfer. Due to its non-adiabatic quantum state transition nature, target electrons are readily captured into high excited states of the ion and subsequently de-excite by emitting X-rays. This process can be represented by the following equation [2-3]:



where  $A^{q+}$ ,  $B$ , and  $\gamma$  denote the projectile ion, target atom/molecule, and X-ray photon, respectively, while  $n$  and  $l$  represent the principal and angular momentum quantum numbers. As seen from Eq. (1), this process encompasses both collision dynamics and structural spectroscopy. Based on momentum and energy conservation, the following dynamical relationship exists between the longitudinal recoil momentum  $P_{r\parallel}$  of the  $B^+$  ion, the reaction energy  $Q$ , and the projectile velocity, as expressed in Eq. (2):

$$P_{r\parallel} = n_c m_e v_p \quad (2)$$

where  $Q$  represents the change in binding energy of the target electron before and after the reaction,  $v_p$  is the projectile ion velocity, and  $n_c$  is the number of captured electrons. Using high-resolution cold target recoil ion momentum spectroscopy, atomic physicists can obtain state-selective relative cross sections and population information for captured electrons, which can then be normalized to total cross sections to yield absolute state-selective cross sections [4]. Spectroscopically, projectile ions in excited states following capture spontaneously radiate during de-excitation, emitting photons. By measuring photon energies and spectral line intensity ratios and considering cascade radiation models, one can also infer ion species and state population information from charge exchange. Therefore, studies of this process not only advance our understanding of multi-center quantum state transition mechanisms in the microscopic world but also have important applications in numerous macroscopic research fields, including X-ray astronomical observations, plasma diagnostics, and ion-irradiated material characterization.

Taking astrophysical environment modeling as an example, observed X-ray emission spectra can be used to identify plasma environments in celestial objects, with their species, composition, temperature, and other physical properties requiring laboratory measurements of the same astrophysical processes to provide benchmarks. For instance, high charge-state ions produced by stellar burning and supernova explosions undergo charge exchange with interstellar neutral atoms and molecules with large reaction cross sections, making this physical process a natural probe for detecting astrophysical environments. Consequently, laboratory-based charge exchange experimental data provide benchmark atomic data for this process.

Here, we illustrate the application of charge exchange in X-ray astronomy. In 1996, Lisse et al. [5] first observed X-ray spectra from comet C/Hyakutake 1996 B2. Subsequently, the ROSAT observatory detected X-rays from five additional comets [6], sparking great interest among astronomers. In 2001, Lisse et al. proposed that the soft X-rays observed from comet C/Hyakutake most likely originated from interactions between solar wind ions such as  $C^{5+}$ ,  $N^{7+}$ ,  $O^{8+}$  and cometary gases [7]. In 2003, Beiersdorfer et al. confirmed the soft X-ray emission mechanism from charge exchange between solar wind ions and neutral atoms/molecules in the cometary coma through laboratory simulations [8]. Cravens et al. predicted that 25-50% of soft X-rays in the heliosphere result from charge exchange between solar wind ions and interstellar neutral atoms/molecules [9], with almost all soft X-ray emission in certain observational directions arising from charge exchange [10]. With advances in astrophysical observations and high-resolution soft X-ray detection technology, soft X-ray emissions have been observed in astrophysical environments such as supernova explosion debris shock waves [11], extragalactic clusters beyond the solar system [12], and star-forming galaxies [13]. When these hot, high charge-state plasma flows are ejected into interstellar space and collide with neutral gases, charge exchange occurs, releasing X-rays that become an important source of cosmic diffuse background X-rays.

The needs of astrophysical observation modeling pose new challenges for laboratory astrophysics research. Laboratory simulation of charge exchange plasma X-ray spectra in astrophysical environments has emerged as a new field. International groups conducting such research include the Chutjian group at NASA's Jet Propulsion Laboratory [14], the Beiersdorfer group at Lawrence Livermore National Laboratory [8,15], the Havener group at Oak Ridge National Laboratory [16], the Crespo group at the Max Planck Institute, and the Hoekstra group at the University of Groningen [17]. These groups primarily focus on developing crystal spectrometers or calorimeter techniques for high-resolution soft X-ray measurements relevant to astrophysical charge exchange, measuring charge exchange X-ray spectra in laboratories and fitting them to astronomical observations to determine high charge-state heavy ion velocities and compositions in astrophysical environments. Another important aspect of laboratory astrophysics research involves modeling astrophysical X-ray spectra using extensive charge exchange atomic data, with current models including ATOMDB [18], Plasma Code [19], and XSPEC [20]. In China, institutions including the Institute of Modern Physics of the Chinese Academy of Sciences, Fudan University, the National Astronomical Observatories, and the Purple Mountain Observatory have gradually initiated research in both aspects, with increasingly close collaboration.

In this paper, we employ the multi-channel Landau-Zener (MCLZ) method to calculate charge exchange cross sections for bare and hydrogen-like C, N, and O ions colliding with hydrogen atoms, and compare them with existing experimental cross-section data. We compare state-selective cross-section data calculated by both MCLZ and fully quantum-mechanical molecular orbital close-coupling

(QMOCC) methods for the  $C^{5+} + H$  system to examine the accuracy of the MCLZ method. Based on the Kronos program package [21-22] and using cascade radiation models, we calculate the charge exchange X-ray spectrum, photon energies, spectral line emission cross sections, and line intensity ratios for  $O^{8+} + H$ . Additionally, we calculate hardness ratios using different  $l$ -distribution models with MCLZ method for  $O^{8+} + H$  and compare the results with those obtained using the recommended cross-section data from Janev [1]. This cross-section data selects appropriate theoretical calculation methods based on collision energy and evaluates the results using experimental cross sections of emission lines. These calculations provide theoretical guidance for our subsequent experimental studies. Due to the lack of charge exchange cross-section data for bare and hydrogen-like ions and gaps in some collision systems, current astrophysical modeling primarily relies on theoretically calculated cross-section data. Although classical theories compute rapidly, they show large deviations from experimental results. Fully quantum-mechanical calculation theories have high computational demands and cannot handle multi-electron collision systems. Therefore, we aim to incorporate high-resolution state-selective cross-section information obtained from laboratory charge exchange experiments into the Kronos program package to improve the accuracy of cascade radiation X-ray spectrum calculations and obtain more precise line intensity ratio information, which will greatly aid in understanding and simulating various astrophysical processes.

## 2 Theoretical Calculations

The Kronos program package primarily consists of two components: charge exchange data and cascade radiation X-ray spectrum calculations [21-22]. Charge exchange data can be generated using methods including MCLZ, classical trajectory Monte Carlo (CTMC), atomic orbital close-coupling (AOCC), molecular orbital close-coupling (MOCC), and QMOCC. Among these, the built-in charge exchange data in Kronos are mainly produced by the MCLZ method, with some cross-section data for certain collision systems calculated using quantum-mechanical methods such as AOCC and MOCC. Based on these state-selective cross-section data, cascade radiation models calculate transition probabilities and branching ratios to obtain X-ray emission spectra. We have developed a multi-parameter fitting Python program that rapidly batch-acquires charge exchange cross-section data and X-ray emission spectra based on the Kronos package. We summarize the Kronos output results, selecting appropriate ion species, collision energies, and energy resolutions for astrophysical environments, then fit them with experimental data from astrophysical X-ray observations to infer ion abundance information in astrophysical environments, as detailed in [23].

The MCLZ method is a classical approach for treating charge exchange problems that computes rapidly and shows reasonable agreement with experimental results in terms of magnitude and trends. Therefore, all calculations in this paper are based on this method. Here we provide a brief introduction to the MCLZ

method. Charge exchange is a problem of multi-quantum-state population. In Landau-Zener theory, let  $p_n$  denote the probability that the collision system remains on the  $A^{q+} + B$  potential curve when passing the  $n$ th avoided crossing point. The transition probability for the collision system at this crossing point,  $R = R_n$ , can be expressed as [24]:

$$P_n = (1 - p_n) \prod_{i=1}^{n-1} p_i \prod_{j=n+1}^N p_j \quad (3)$$

where  $N$  is the number of avoided crossing points,  $1 \leq n \leq N$ , and  $n$  corresponds to the number of final states after electron transition. In the above expression, transition probabilities  $p_i$  with indices greater than  $N$  are zero. Landau and Zener independently derived the transition probability expression [25-26] as follows:

$$p_n = \exp\left(-\frac{2\pi H_{12}(R_n)^2}{v_{rad}(R_n)\Delta F(R_n)}\right) \quad (4)$$

where  $H_{12}$  is the coupling matrix element describing the radial coupling strength between initial and final states,  $v_{rad}$  is the radial velocity, and  $\Delta F$  is the magnitude of the difference in derivatives of the initial and final potential curves, expressed as:

$$\Delta F = \left| \frac{d}{dR}(V_1 - V_2) \right|_{R=R_n} \quad (5)$$

The Landau-Zener transition probability at crossing points is valid under the condition that the transition region  $\delta R = |H_{12}/\Delta F|_{R=R_n}$  is much smaller than the spacing between two adjacent avoided crossing points [27]. All variables mentioned above refer to values at  $R = R_n$  [27-28]. The radius of avoided crossing points can be estimated from the incident channel being constant and the exit channel being purely Coulombic.

For two-state problems with only one crossing point, as the incident ion approaches the target atom, the distance between the two nuclei gradually decreases. The electron passes the avoided crossing point twice during approach and departure, with the final capture probability at the crossing point given by:

$$P_n(b) = 2p_n(1 - p_n) \quad (6)$$

The reaction cross section is obtained by integrating the transition probability over impact parameters:

$$\sigma_n = 2\pi \int P_n(b) b db \quad (7)$$

When using the MCLZ method to calculate cross sections, all possible capture channels must be considered and the positions of avoided crossing points calculated. This process requires accurate energy level information for these electronic states. For highly charged helium-like ions such as  $\text{Fe}^{24+}$ , energy level information for high principal quantum numbers  $n$  is often lacking. Therefore, quantum defects must be considered based on the Rydberg formula to estimate electronic state energy levels:

$$E_{nl} = E_0 \left( 1 - \frac{1}{n^{*2}} \right) \quad (8)$$

where  $n^*$  is the effective quantum number obtained from Eqs. (9) and (10):

$$n^* = n - \mu_l \quad (9)$$

$$\mu_l = \delta \quad (10)$$

Here  $\mu_l$  is called the quantum defect, calculated from Eq. (10), arising from the penetration effect of valence electron orbitals. In Eq. (10), the variation trend of  $\delta$  values is estimated from known energy levels and then applied to highly excited ionic states to obtain electronic state energies  $E_{nl}$ .

When using the MCLZ method to generate charge exchange cross sections for bare projectile ions, the angular quantum number  $l$  of the product ion after reaction is degenerate. Landau-Zener theory requires that avoided crossing points be sufficiently separated. To obtain  $nl$ -resolved state-selective cross sections, we must apply  $l$ -distribution models. The  $n$ -resolved charge exchange cross sections are multiplied by appropriate  $l$ -distribution functions to obtain  $nl$ -resolved state-selective cross sections. Commonly used  $l$ -distribution models include statistical distribution (Stat), low-energy distribution (Low) [29], modified low-energy distribution (LowMod) [30], separable distribution (Sep), and Landau-Zener distribution (LZ) [31].

The statistical and low-energy distributions are commonly used. According to Krasnopolsky [29], the statistical model applies when ion energies exceed 10 keV/u, where angular quantum numbers  $l = n - 1$  dominate capture. The low-energy model, proposed by Abramov et al. [32], applies to energies below 100 eV/u, where for capture with  $n < 8$ ,  $l = 1$  dominates and  $l$  gradually increases with  $n$ .

Following charge exchange, electrons are typically captured into excited states of the ion, whose unstable nature causes rapid de-excitation through cascade radiation. The cascade radiation model considers all dipole-allowed transition channels with  $\Delta l = \pm 1$  and  $\Delta S = 0$ , calculating transition probabilities  $A_{n,l \rightarrow n',l'}$ , i.e., Einstein spontaneous emission coefficients. Combining the population of electronic states after capture with all possible cascade radiation transition paths

and summing the total probability for any transition yields spectral line intensity ratios. Lyman series lines correspond to transitions  $n \geq 2 \rightarrow n = 1$  and directly reflect information about high charge-state ion species. High charge-state ions in astrophysical environments de-excite and emit photons, with Lyman series line energies primarily in the X-ray regime. Using X-ray detectors or microcalorimeters, the origins of these spectral lines can be resolved.

### 3 Results and Discussion

To examine the reliability of charge exchange cross sections produced by the MCLZ method, we compare total cross sections for bare and hydrogen-like C, N, and O ions colliding with H atoms calculated by the MCLZ method with experimental charge exchange measurements. Hydrogen atom, being the simplest single-electron system, requires consideration of only single-electron capture processes in charge exchange collisions, without contributions from multi-electron capture processes. Furthermore, the MCLZ method shows good agreement with experimental results for single-electron capture problems, while multi-electron capture processes requiring consideration of numerous incident and exit channels lead to larger computational deviations.

[Figure 1: see original paper] shows total cross-section data from charge exchange experiments by Draganić and Meyer [34]. The red lines represent MCLZ-calculated total cross sections. We find that for the  $C^{5+} + H$  system, experimental cross sections are significantly higher than MCLZ-calculated cross sections across the calculated energy range. For  $C^{6+} + H$ ,  $N^{6+} + H$ , and  $O^{8+} + H$  collision systems, experimental cross sections decrease with decreasing collision energy in the low-energy region, while MCLZ calculations predict this decreasing trend but with slower cross-section variations that deviate from experimental results. For the  $O^{7+} + H$  system, MCLZ predicts increasing cross sections at low energies while experimental cross sections remain essentially energy-independent. The  $N^{7+} + H$  system shows good agreement between experimental and theoretical cross sections.

For solar wind ions, typical velocity ranges are 400-1200 km/s [35], with velocities below 400 km/s termed slow solar wind and those above 1000 km/s fast solar wind. Portions exceeding 750 km/s may originate from high-latitude solar coronal holes, decreasing below slow solar wind levels in cometary and planetary bow shocks [36]. We find that within the solar wind energy range, except for the  $C^{5+} + H$  system where experimental cross sections deviate significantly from MCLZ calculations, total cross-section data from the MCLZ method agree well with experimental results for other systems, providing convenience for simulating solar wind ion charge exchange processes.

Through comparison with experimental data, we demonstrate the reliability of the MCLZ method for calculating single-capture total cross sections in the solar wind energy range. Further, we require  $nl$ -resolved state-selective cross sections to normalize relative state-selective cross sections using total cross

sections, thereby obtaining absolute state-selective cross sections for calculating X-ray spectra of different projectiles. For high charge-state ions forming hydrogen-like and helium-like ions after charge exchange, state-selective cross sections resolved by principal quantum number  $n$  can be measured experimentally using cold target recoil ion momentum spectroscopy. Since the angular momentum quantum number  $l$  of hydrogen-like ions after reaction is degenerate, distinguishing electronic states with different angular quantum numbers in energy spectra is extremely difficult. The common approach is to superimpose  $l$ -distribution functions on  $n$ -resolved state-selective cross sections. For helium-like ions, some configurations also exhibit energy degeneracy. Moreover, current cold target recoil ion momentum spectrometers typically have energy resolutions of 3-5 eV for reaction energy  $Q$ , making it difficult to resolve angular quantum numbers  $l$  for high charge-state hydrogen-like and helium-like ions. Theoretically, quantum-mechanical charge exchange theories typically describe charge exchange processes more accurately, consistent with experiments. Therefore, we compare state-selective cross sections calculated by MCLZ and QMOCC methods to examine the reliability of the MCLZ method.

[Figure 2: see original paper] presents state-selective cross sections for  $C^{5+} + H$  calculated by QMOCC [37] and MCLZ methods, with Figs. 2(a) and 2(b) corresponding to capture into principal quantum numbers  $n = 3$  and  $n = 4$ , respectively. In this collision system and energy range, capture into  $n = 3$  and  $n = 4$  are the dominant channels, so we only list and compare state-selective cross sections for these principal quantum numbers. In Fig. 2(a), we observe that MCLZ-calculated cross sections for capture into  $n = 3$  increase with collision velocity, with larger cross sections for capture into higher angular momentum states. Cross sections for capture into low angular momentum states increase rapidly with collision velocity, showing greater sensitivity to projectile velocity changes. The 3d (3D) state shows a decreasing trend above 10 keV/u. QMOCC-calculated cross sections for the 3s state decrease above projectile energies of 6 keV/u, 3p state cross sections decrease above 10 keV/u, while 3d state cross sections increase throughout the energy range and plateau.

Fig. 2(b) shows state-selective cross sections for  $n = 4$  calculated by both methods. QMOCC-calculated cross sections are overall larger than MCLZ-calculated cross sections, with QMOCC state-selective cross sections showing little variation in the considered energy range, while MCLZ-calculated cross sections decrease monotonically within the considered energy range. Comparing Figs. 2(a) and 2(b), we find that as projectile collision velocity increases, state-selective cross sections for  $n = 3$  increase relative to those for  $n = 4$ , implying that electrons are more easily captured into inner-shell electronic states. Similar results are corroborated in most charge exchange experiments [38].

Through comparison of state-selective cross sections calculated by QMOCC and MCLZ methods, we find that MCLZ-calculated cross sections for this collision system are lower than QMOCC results, and the two methods exhibit different trends in state-selective cross sections as a function of velocity. This creates

difficulties for modeling astrophysical charge exchange X-ray spectra. To reduce this impact, we can normalize MCLZ-calculated  $nl$ -resolved state-selective cross sections using experimentally obtained total cross-section data to minimize effects from total cross-section discrepancies in fitting processes. On the other hand,  $n$ -resolved state-selective cross sections can be obtained using cold target recoil ion momentum spectroscopy, which will further reduce theoretical method errors.

[Figure 3: see original paper] shows the Lyman series X-ray spectrum from  $O^{8+} + H$  charge exchange calculated using the Kronos package. Fig. 3(a) presents the spectrum with 10 eV resolution. The peak at 653 eV arises from Lyman  $\alpha$ , 774 eV from Lyman  $\beta$ , 817 eV from Lyman  $\gamma$ , and 836 eV from Lyman  $\delta$ . Since capture cross sections for channels with  $n \geq 6$  are very small, contributions from  $n \geq 6$  can be neglected. Based on current astrophysical observation satellite spectrometer systems for observing astronomical X-ray spectra, such as Chandra, with resolutions of 50-100 eV [7,39], Fig. 3(b) calculates the X-ray spectrum with 50 eV resolution. Since spectral line energy spacings are smaller than the resolution, Lyman  $\beta$ - $\delta$  lines in Fig. 3(b) can no longer be resolved. In the energy region below 200 eV, abundant soft X-ray and extreme ultraviolet photons are also present, primarily produced by cascade radiation to higher principal quantum numbers  $n$ .

Janev and Winter proposed that the principal quantum number  $n_{max}$  with maximum capture probability for low-energy ion charge exchange is given by Eq. (12):

$$n_{max} \sim \frac{q}{\sqrt{2q}} \quad (12)$$

where  $q$  is the ion charge state. This formula yields  $n_{max} \approx 5$  for  $O^{8+} + H$  charge exchange. However, this predictive formula does not include velocity-dependent terms and cannot describe how capture channels vary with projectile velocity.

lists photon energies, spectral line emission cross sections, and line intensity ratios for  $O^{8+} + H$  charge exchange at 1000 eV/u calculated in this work. Line intensity ratios are defined as relative ratios to Lyman  $\alpha$ . We find that the Lyman  $\delta$  line intensity ratio is much stronger than neighboring lines, indicating that MCLZ calculations predict dominant capture into the  $n = 5$  electronic state. In [Figure 4: see original paper], we show line intensity ratios Lyman  $\beta$ /Lyman  $\alpha$ , Lyman  $\gamma$ /Lyman  $\alpha$ , and Lyman  $\delta$ /Lyman  $\alpha$  as functions of collision velocity calculated by different methods [40-41].

[Figure 5: see original paper] shows hardness ratios of X-ray spectra as functions of collision velocity calculated using different  $l$ -distribution functions with MCLZ method cross sections. We find that hardness ratios from different  $l$ -distribution functions vary considerably. Hardness ratios calculated using

MCLZ + separable distribution and Janev's recommended cross sections [1] decrease with increasing collision velocity, while those from other distribution functions increase with collision velocity. MCLZ + low-energy distribution yields large hardness ratios due to its maximum population at angular momentum  $l = 1$ . Based on velocity matching in charge exchange, relative cross sections for capture into inner shells increase with velocity. We can therefore infer that when angular momentum population shows little sensitivity to velocity, hardness ratios will exhibit a decreasing trend with increasing collision velocity. In Fig. 5, hardness ratios from different  $l$ -distribution functions range from 0.2 to 1.3, indicating that  $l$ -distribution functions can significantly affect spectral properties, making accurate  $l$ -distribution information crucial.

We compared total cross sections for bare and hydrogen-like C, N, and O ions colliding with H atoms with MCLZ-calculated total cross sections. MCLZ-calculated cross sections for  $C^{5+} + H$  are lower than experimental cross sections across the entire energy range. For  $C^{6+} + H$ ,  $N^{6+} + H$ , and  $O^{8+} + H$ , MCLZ-calculated cross sections show large deviations from experimental cross sections at low energies, with experimental cross sections decreasing faster than theoretical predictions. MCLZ-calculated cross sections for  $O^{7+} + H$  increase with decreasing collision energy at low energies. MCLZ-calculated cross sections for  $N^{7+} + H$  show good agreement with experimental cross sections.

We compared  $nl$ -resolved state-selective cross sections for  $C^{5+} + H$  ( $n = 3, 4$ ) calculated by MCLZ and QMOCC methods as functions of collision velocity. QMOCC results are larger than MCLZ results and show different velocity dependence trends. This will introduce errors when applying the MCLZ method to astrophysical charge exchange X-ray modeling. Using the Kronos package, we calculated the X-ray spectrum and various line intensity ratios for  $O^{8+} + H$  charge exchange at 1000 eV/u, analyzing spectral properties based on post-capture state populations. We further calculated line intensity ratios and hardness ratios at different collision energies and analyzed their trends. Comparisons show that hardness ratios from Janev's recommended cross-section data and MCLZ with separable distribution exhibit decreasing trends, while those from other MCLZ distribution functions show increasing trends. By considering velocity dependence of capture state-selective properties, we conclude that different  $l$ -distribution functions in the MCLZ method produce large differences in hardness ratios, making calculated results highly sensitive to  $l$ -distribution functions. This demands development of more accurate theoretical calculation methods and high-resolution experimental techniques. In the future, we will conduct high-resolution state-selective charge exchange experiments using recoil ion momentum spectroscopy techniques to provide more accurate state-selective cross-section data for astrophysical environment simulations.

## References

- [1] JANEV R, PHANEUF R, TAWARA H, et al. Atomic Data and Nuclear Data Tables, 1993, 55(2): 201[2023-04-21]. DOI: 10.1006/adnd.1993.1021.

- [2] DÖRNER R, MERGEL V, JAGUTZKI O, et al. *Physics Reports*, 2000, 330(2): 95. <https://www.sciencedirect.com/science/article/pii/S037015739900109X>. DOI: [https://doi.org/10.1016/S0370-1573\(99\)00109-X](https://doi.org/10.1016/S0370-1573(99)00109-X).
- [3] ULLRICH J, MOSHAMMER R, DORN A, et al. *Reports on Progress in Physics*, 2003, 66(9): 1463. <https://dx.doi.org/10.1088/0034-4885/66/9/203>.
- [4] HAN J, WEI L, WANG B, et al. *ApJS*, 2021, 253(1): 6[2023-10-18]. DOI: 10.3847/1538-4365/abde44.
- [5] LISSE C M, DENNERL K, ENGLHAUSER J, et al. *Science*, 1996, 274(5285): 205. DOI: 10.1126/science.274.5285.205.
- [6] DENNERL K, ENGLHAUSER J, TRÜMPER J. *Science*, 1997, 277(5332): 1625. <https://www.science.org/doi/abs/10.1126/science.277.5332.1625>.
- [7] LISSE C M, CHRISTIAN D J, DENNERL K, et al. *Science*, 2001, 292(5520): 1343. DOI: 10.1126/science.292.5520.1343.
- [8] BEIERSDORFER P, BOYCE K R, BROWN G V, et al. *Science*, 2003, 300(5625): 1558. DOI: 10.1126/science.1084373.
- [9] CRAVENS T E. *Astrophys J Lett*, 2000, 532(2): L153. DOI: 10.1086/312574.
- [10] KOUTROUMPA D, LALLEMENT R, RAYMOND J C, et al. *Astrophys J Lett*, 2009, 696: 1517. DOI: 10.1088/0004-637X/696/2/1517.
- [11] KATSUDA S, TSUNEMI H, MORI K, et al. *ApJ*, 2011, 730: 24. DOI: 10.1088/0004-637X/730/1/24.
- [12] FABIAN A C, SANDERS J S, WILLIAMS R J R, et al. *MNRAS*, 2011, 417(1): 172. DOI: 10.1111/j.1365-2966.2011.19034.x.
- [13] LIU J, MAO S, WANG Q D. *Monthly Notices of the Royal Astronomical Society: Letters*, 2011, 415(1): L64[2023-11-15]. DOI: 10.1111/j.1745-3933.2011.01079.x.
- [14] MACHACEK J, MAHAPATRA D, SCHULTZ D, et al. *Physical Review A*, 2014, 90: 052708. DOI: 10.1103/PhysRevA.90.052708.
- [15] BEIERSDORFER P, OLSON R E, BROWN G V, et al. *Phys Rev Lett*, 2000, 85: 5090. <https://link.aps.org/doi/10.1103/PhysRevLett.85.5090>.
- [16] HAVENER C C, HUQ M S, KRAUSE H F, et al. *Phys Rev A*, 1989, 39: 1725. <https://link.aps.org/doi/10.1103/PhysRevA.39.1725>.
- [17] BODEWITS D, HOEKSTRA R. *Phys Rev A*, 2007, 76: 032703. <https://link.aps.org/doi/10.1103/PhysRevA.76.032703>.
- [18] FOSTER A R, JI L, SMITH R K, et al. *The Astrophysical Journal*, 2012, 756(2): 128. <https://dx.doi.org/10.1088/0004-637X/756/2/128>.
- [19] LIYI G, KAASTRA J, RAASSEN A, et al. *Astronomy and Astrophysics*, 2015, 584. DOI: 10.1051/0004-6361/201527634.
- [20] Arnaud K A. XSPEC: The First Ten Years[C]//Jacoby G H, Barnes J. *Astronomical Society of the Pacific Conference Series: volume 101 Astronomical Data Analysis Software and Systems V*. 1996: 17.
- [21] CUMBEE R S, LIU L, LYONS D, et al. *Monthly Notices of the Royal Astronomical Society*, 2016, 458(4): 3554. <https://doi.org/10.1093/mnras/stw527>.
- [22] MULLEN P D, CUMBEE R S, LYONS D, et al. *The Astrophysical Journal Supplement Series*, 2016, 224(2): 31. <https://dx.doi.org/10.3847/0067-0049/224/2/31>.
- [23] ZHANG R T, LIAO T, ZHANG C J, et al. *Monthly Notices of the Royal As-*

- tronomical Society, 2023, 520(1): 1417. <https://doi.org/10.1093/mnras/stad040>.
- [24] SALOP A, OLSON R E. Phys Rev A, 1976, 13: 1312. <https://link.aps.org/doi/10.1103/PhysRevA.13.1312>.
- [25] LANDAU L, LIFSHITZ E. 19 - On the theory of energy transfer during collisions. III Reprinted from Zhurnal Eksperimental' noi i Teoreticheskoi Fiziki 18, Part 8, 750, 1948.[M/OL]//PITAEVSKI L. Perspectives in Theoretical Physics. Amsterdam: Pergamon, 1992: 287. DOI: 10.1016/B978-0-08-036364-6.50024-7.
- [26] Zener C. Proceedings of the Royal Society of London Series A, 1932, 137(833): 696. DOI: 10.1098/rspa.1932.0165.
- [27] JANEV R K, BELIĆ D, BRANSDEN B H. Phys Rev A, 1983, 28: 1293. <https://link.aps.org/doi/10.1103/PhysRevA.28.1293>.
- [28] ZHU X. Kinematically complete investigation of the dynamics in slow he2+ on he collisions(in chinese)[Z]. 2006.
- [29] KRASNOPOLSKY V, GREENWOOD J, STANCIL P. Space Science Reviews, 2004, 113: 271. DOI: 10.1007/s11214-005-6263-2.
- [30] Smith R K, Foster A R, Edgar R J, et al. apj, 2014, 787(1): 77. DOI: 10.1088/0004-637X/787/1/77.
- [31] JANEV R, WINTER H. Physics Reports, 1985, 117(5): 265. <https://www.sciencedirect.com/science/article>
- [32] Abramov V A, Baryshnikov F F, Lisitsa V S. Soviet Journal of Experimental and Theoretical Physics Letters, 1978, 27: 464.
- [33] DRAGANIĆ I N, SEELY D G, HAVENER C C. Phys Rev A, 2011, 83: 054701. <https://link.aps.org/doi/10.1103/PhysRevA.83.054701>.
- [34] MEYER F W, HOWALD A M, HAVENER C C, et al. Phys Rev A; (United States), 1985, 32:6(1). <https://www.osti.gov/biblio/6388722>. DOI: 10.1103/PhysRevA.32.3310.
- [35] BODEWITS D, HOEKSTRA R, SEREDYUK B, et al. The Astrophysical Journal, 2006, 642(1): 593. <https://dx.doi.org/10.1086/500595>.
- [36] GOLDSTEIN B E, NEUGEBAUER M, BALSIGER H, et al. Giotto-IMS observations of ion-flow velocities and temperatures outside the magnetic cavity of comet P/Halley[M/OL]//GREWING M, PRADERIE F, REINHARD R. Exploration of Halley' s Comet. Berlin, Heidelberg: Springer Berlin Heidelberg, 1988: 174[2023-11-15]. DOI: 10.1007/978-3-642-82971-0\_{32}.
- [37] NOLTE J L, STANCIL P C, LIEBERMANN H P, et al. J Phys B: At Mol Opt Phys, 2012, 45(24): 245202[2023-06-19]. DOI: 10/gr766t.
- [38] RYUFUKU H, SASAKI K, WATANABE T. Phys Rev A, 1980, 21(3): 745[2023-07-06]. DOI: 10.1103/PhysRevA.21.745.
- [39] BROMLEY S J, PINDZOLA M, BODEWITS D, et al. The Astrophysical Journal Supplement Series, 2022, 262(2): 47. <https://dx.doi.org/10.3847/1538-4365/ac8977>.
- [40] PINDZOLA M S, FOGLE M, STANCIL P C. J Phys B: At Mol Opt Phys, 2018, 51(6): 065204[2023-04-21]. DOI: 10.1088/1361-6455/aaae5f.
- [41] SHIPSEY E J, GREEN T A, BROWNE J C. Phys Rev A, 1983, 27(2): 821[2023-07-03]. DOI: 10.1103/PhysRevA.27.821.

*Note: Figure translations are in progress. See original paper for figures.*

*Source: ChinaXiv – Machine translation. Verify with original.*